

EFFECT OF PRANDTL NUMBER ON TURBULENT HEAT TRANSFER OF CORRUGATED TRAPEZOIDAL PLATE HEAT EXCHANGERS USING NANOFLUIDS

Elif Büyük Öğüt

Kocaeli University Hereke MYO, 41800 Hereke, Kocaeli
elif.ogut@kocaeli.edu.tr

Seda Dilki

Kocaeli University Institute of Science, Kocaeli
seda_dilki@hotmail.com

Abstract: In this study, fully developed turbulent flow and heat transfer behavior of water, ethylene glycol, mercury and propane based nanofluids in a corrugated trapezoidal plate heat exchanger have been numerically investigated. A constant heat flux was applied to the heat exchanger and the constant heat flux was chosen to be $6 \text{ kW} / \text{m}^2$, volume fractions $\phi=0\%-4\%$, diameter $d = 20 \text{ nm}$ and Al_2O_3 was selected as nanoparticle. The Reynolds number varies from 6000 to 20000. Geometric parameters of the corrugated trapezoidal channel, trapezoidal height $e=5\text{mm}$, trapezoidal pitch $Pe=12\text{mm}$, width of the top trapezoidal channel $w=3\text{mm}$. Executive equations have been solved with Ansys Fluent programme. The velocity distribution, temperature contours, pressure drop, average Nu number and thermal-hydraulic performance have been analyzed and presented. The effects of nanofluids have been examined on heat and flow fields and it has been observed that the heat transfer increases together with the nanoparticle volume concentration. When the nanofluid is used in a forced convection, the amount of heat transfer increases as the Prandtl number increases. The highest value of the average Nusselt number was obtained in the ethylene glycol-based nanofluid, and the lowest value was obtained in the mercury-based nano-fluid. Results show that the use of nanofluid in the corrugated trapezoidal channel increases the thermal performance of systems and thus contributes to the design of more compact heat exchanger.

Key words: Heat exchanger, corrugated trapezoidal plate, nanofluid, Prandtl number, CFD

Introduction

Heat transfer by means of a fluid is used in many areas, such as heat exchangers, solar collectors, refrigerators, automobiles, cooling of electronic devices, power plants, and many other engineering fields. There is a need to develop advanced heat transfer fluids to improve compact and performance heat exchangers with high thermal conductivity and to meet needs of industry. However, since the base fluids such as air, water, oil, ethylene glycol used for convective heat transfer have very low thermal conductivity, they can not meet the desired properties in today's technology. One of the techniques used for increasing the heat transfer characteristics of heat transfer fluids is the addition of solid particles whose thermal conductivities are higher than base fluids. (Lee and Choi, 1999). The discovery of nanofluids, a new type of suspension in which less than 100 nanometers of solid particles (metal, metal oxide, carbon nanotube) are concerned, have recently increased their use as heat transfer fluids as a result of recent work. The reason for this increase is that nanoparticles have high thermal conductivity values even at very small nanoparticle concentrations (Choi, 1995). Copper, silver, copper oxide, titanium oxide and aluminum oxide are usually used as the nanoparticle. Koblinski et al. (2002) the significant increase in the heat transfer ability of nanofluids is due to factors such as the Brownian motion of the solid particles, the liquid layer at the molecular level at the liquid solid common surface, the nature of the heat transfer mechanism, and nanoparticle collapse. The most important parameter related to the heat transfer in nanofluids is heat conduction ability.

The use of corrugated plate can increase appropriately thermal performance and compactness. The use of a corrugated channel results in a more complex flow structure and improves heat transfer to two or three times that of a conventional straight channel. (Islamoğlu, 2003). Many researchers have developed strategies to reduce the system size of traditional fluid passing through a various cross-section-shaped channel and to improve system performance. They pointed out that wave angle and channel height affect temperature distribution and flow rate significantly. Tanda (2007) has made an experimental study on forced convection in a rectangular channel and V-shaped broken ribbed and transverse rectangular channels. Kwon et al. (2008) have made experimental and numerical studies on various wave-angle rectangular wave pipes. When the performance factor (1.8) and Reynolds

number were 1000, the highest level was found at 100. Naphon (2009), has expressed that corrugated channel arrangements and channel geometries have improved heat transfer performance by increasing surface area and accelerating vortex formation in the flow.

There are many studies in the literature on the thermal performance of water-based nanofluids for plate heat (PHE) exchangers. Pantzali et al. (2009) studied experimentally the effects of 4% CuO nanofluids on the performance of commercial herring-one-type plate heat exchanger (PHE). The experimental data confirmed that besides the physical properties, the type of flow inside the heat exchanging equipment also affects the efficacy of a nanofluid as coolant. The fluid viscosity seems also to be a crucial factor for the heat exchanger performance. Heidary ve Kermani (2010) reported that the addition of 10% Cu-nanoparticles enhances the heat exchange by 25%. Suspension of solid particles in a traditional fluid is another effective passive technique because it effectively enhances the thermophysical properties of the fluid. For this reason, the effect of various types of nanofluids on the performance of different geometries has been tested experimentally and numerically compared to that of the base fluids. Ahmed et al. (2011), explored numerically the laminar forced convection of flow and heat transfer enhancement in a wavy and trapezoidal channel using a Cu-water nanofluid with nanoparticle volume fraction from 0% to 5%. The friction coefficient and Nusselt number increase as the amplitude of the wavy channel increases. As the nanoparticle volume fraction increases, the Nusselt number significantly increases along with a slight increase in the friction coefficient. It was found that the trapezoidal channel has the highest Nusselt number and followed by the sinusoidal, triangular and straight channel. Tiwari et al. (2014) studied numerically fluid flow characteristics of CeO₂-water and Al₂O₃-water nanofluids flowing in a chevron corrugated-plate heat exchanger (PHE). It was found that the use of nanofluid as alternate coolant reduces the pumping cost as it delivers more heat transfer for the same pressure drop as that in the case of water as coolant. Ahmed et al. (2014), convective heat transfer of SiO₂-water nanofluid flow in channels with different shapes is numerically and experimentally have studied over Reynolds number ranges of 400–4000, it is observed that the trapezoidal-corrugated channel has the highest average Nusselt number, pressure drop and heat transfer enhancement followed by the sinusoidal-corrugated channel and straight channel. Rostami (2015) numerically investigated the convective heat transfer of nanofluid flow in a sinusoidal-wavy channel under constant heat flux. Numerical results were obtained for Reynolds numbers range of 100–250 and nanoparticle volume fraction range of 0–10%. The two types of the base fluids such as water and ethylene glycol with Al₂O₃ nanoparticles were considered. Nusselt number and friction factor increased with the increasing of Reynolds number and nanoparticles volume fraction. In addition, the Nusselt number and friction factor of Al₂O₃- ethylene glycol nanofluid were higher than those of the Al₂O₃-water nanofluid. Esmaeili et al. (2010) focused on the alumina nanofluid flow in sinusoidal wavy channel. In this study, the boundary condition was applied as a constant heat flux on the channel walls. The governing equations were solved using finite volume method. The results showed that the nanoparticles addition to the basefluid may significantly increase the heat transfer enhancement, but the wall shear stress also increased. It was also found that at a given nanoparticle fractions, the Nusselt number values at high Reynolds number was higher than those at low Reynolds number. Heidary and Kermani (2012) have studied the laminar flow and heat transfer of nanofluid in sinusoidal-wall channel using finite volume approach. The results indicated that the heat transfer is enhanced by 50% with the increasing of nanofluid volume concentrations of copper as compared to water. On other hand, there was a slight effect of nanoparticles suspension on the skin friction coefficient. Ozbolat and Sahin (2007) have studied the thermal flow of Al₂O₃ in eight wave channel. The wavelength and the amplitude of the wavy channel were 28 mm and 3.5 mm, respectively. The upper and the lower walls of the wavy channel were maintained at uniform wall temperature condition. Tanda (2010) investigated the effect of four different pitch-to-height ratios (p/e) including 6.66, 10.0, 13.33, and 20.0, on heat transfer in a rectangular channel with one-ribbed wall and two-ribbed wall. Results showed that p/e = 13.33 was slightly preferable for the 1RW case (especially at the highest Re values) while a smaller p/e value (p/e=6.66–10) gave the best performance for the 2RW case. Singh et al. carried out an investigation on the effect of flow-attack-angle (α) on thermo-hydraulic performance of rectangular ducts roughened with a new configuration of 'V-down rib having gap' on one wide wall. The results showed the best flow-attack-angle (α) was from 30° to 75°.

In this study, fully developed turbulent flow and heat transfer behavior of water, ethylene glycol, mercury and propane based nanofluids in a corrugated trapezoidal plate heat exchanger have been numerically investigated. The effects of Prandtl number on the turbulent flow and heat transfer of the effects of Al₂O₃ nanoparticles at different volume fractions (ϕ = 0% - 4%) under constant heat flow (6 kW / m²).

Physical Model

In this study, the two-dimensional geometry of the trapezoidal channel plate examined in the analyzes is shown in Fig 1. Selected geometric parameters; the channel height is H=12,5 mm, the channel length is L=95 mm, the floor height of trapeze channel is b=4 mm, trapezoidal height is e= 5 mm, trapezoidal pitch is Pe= 12 mm, width of the

top trapezoidal channel is $w=Pe/4= 3$ mm. To ensure a fully-developed flow, the length of each adiabatic wall section before and after the corrugated section is set to be 250 and 100 mm, respectively. In the analyzes, the nanoparticle and the fluid are assumed to be at the same velocity and thermodynamic equilibrium. Water, ethylene glycol, mercury and propane are used as the base fluid, and also Al_2O_3 is used as the nanoparticle. Nanofluid suspension was obtained by adding Al_2O_3 nanoparticles at 20 nm diameter and different volume fractions 0%, 1%, 2%, 3%, 4% in water, ethylene glycol, mercury and propane base fluids. The thermophysical properties of the base fluids and nanoparticle are given in Table 1.

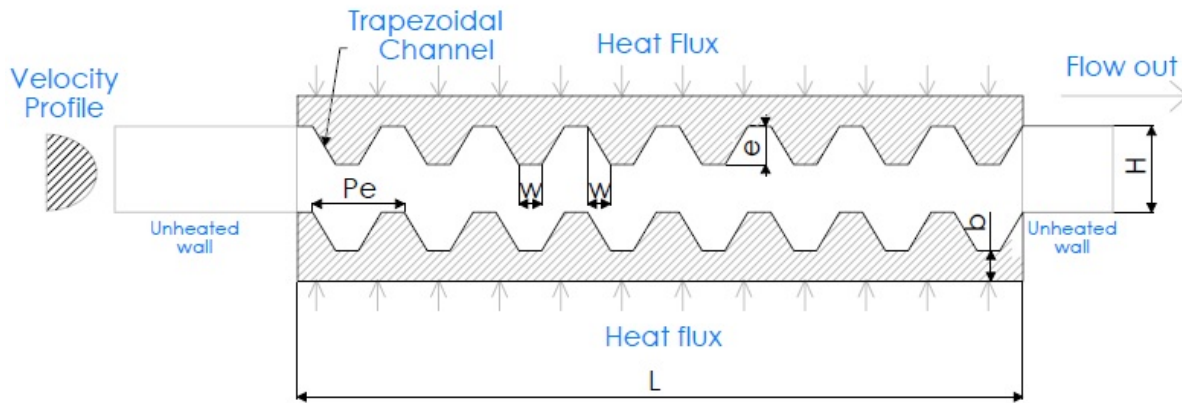


Fig.1. Schematic diagram of the corrugated trapezoidal channel.

Table 1. Thermophysical properties of base fluids and nanoparticle.

Properties	Mercury	Propane	Water	EG	Al_2O_3
ρ (kg/m ³)	13534	492,2	997,1	1132	3970
C_p (J/kgK)	139,4	2742	4180	2349	765
k (W/mK)	8,52	0,0928	0,613	0,258	40
μ kg/m.s)	0,00153	0,000097	0,000891	0,0151	--
β (1/K)	0,000181	0,00337	0,00021	0,00057	0,000024
Pr	0.0251	2.87	6.07	137.48	-

Mathematical Model

In this study, the single-phase and the $k-\epsilon$ standard turbulence model have been used to solve the turbulent heat transfer and flow characteristics. The executive equations can be written in the following form;

The continuity equation is;

$$\frac{\partial}{\partial x_i}(\rho u_i) = 0 \tag{1}$$

The momentum equation is;

$$\frac{\partial}{\partial x_j}(\rho u_i u_j) = -\frac{\partial p}{\partial x_i} + \frac{\partial}{\partial x_j} \left[\mu \left(\frac{\partial u_i}{\partial x_j} + \frac{\partial u_j}{\partial x_i} - \frac{2}{3} \delta_{ij} \frac{\partial u_k}{\partial x_k} \right) \right] + \frac{\partial}{\partial x_j} (-\rho \overline{u_i u_j}) \tag{2}$$

The energy equation is;

$$\frac{\partial}{\partial x_i} [u_i (\rho E + p)] = \frac{\partial}{\partial x_j} \left[\left(k + \frac{C_p \mu_t}{Pr_t} \right) \frac{\partial T}{\partial x_j} + u_i (\tau_{ij})_{\text{eff}} \right] \quad (3)$$

The symbols ρ , μ , u' , u_i , u_j , are fluid density, viscosity, fluctuated velocity, axial velocity and the velocity in vertical direction respectively. The term $\overline{\rho u_i' u_j'}$ is turbulent shear stress where Pr_t is the turbulent Prandtl number (0.85) ve $(\tau_{ij})_{\text{eff}}$ is the deviatoric stress tensor.

Boundary Conditions

The boundary conditions imposed at the external corrugated channel are no-slip, and with constant heat flux, whereas the flat walls are thermally insulated. The velocity boundary condition is applied at the inlet, whereas the pressure boundary condition is used at the outlet. The boundary conditions for a steady-state, 2D flow rate are as follows:

At the wall; $u = 0, v = 0, q = q_{\text{wall}} \quad (4)$

At the inlet; $u = u_{\text{in}}, v = 0, T = T_{\text{in}} \quad (5)$

The average heat transfer coefficient along the corrugated trapezoidal channel h_c , can be calculated from the average heat transfer rate obtained from;

$$Q_{\text{ave}} = h_c A_c (\Delta T_{\text{LMTD}}) \quad (6)$$

$$\Delta T_{\text{LMTD}} = \frac{(T_{s,\text{ave}} - T_{\text{nf,ave,in}}) - (T_{s,\text{ave}} - T_{\text{nf,ave,out}})}{\ln(T_{s,\text{ave}} - T_{\text{nf,ave,in}} / T_{s,\text{ave}} - T_{\text{nf,ave,out}})} \quad (7)$$

The average Nusselt number is;

$$Nu_{\text{ave}} = \frac{h_c H_{\bar{x}}}{k L_{\text{corr}}} \quad (8)$$

The inlet velocity and Reynolds number is;

$$u_{\text{in}} = \frac{Re \mu}{\rho D_H}, \quad Re = \frac{\rho D_H u_{\text{in}}}{\mu} \quad (9)$$

The hydraulic diameter is;

$$D_H = \frac{4A_{\text{cross}}}{P} \quad (10)$$

The Fanning friction factor is;

$$C_{\text{fx}} = \frac{2\tau_s}{\rho u_{\text{in}}^2} \quad (11)$$

The Darcy friction factor is;

$$f = 4C_{\text{fx}} \quad (12)$$

The pressure drop is;

$$\Delta p = f \frac{L \rho u_{\text{in}}^2}{2D_H} \quad (13)$$

The values used in analyzes are taken as $A_c=0.278\text{m}^2$, $H=0.0125\text{m}$, $L_{\text{corr}}=0.095\text{m}$, $\bar{x}=0.05\text{m}$, $D_H=0.025\text{m}$.

Models used for thermophysical properties of nanofluid

The proposed models for viscosity and thermal conductivity of the nanofluid are as follows. In these equations ϕ is the volumetric ratios of the solid particles, while the subindices nf, f and p represent the nanofluid, base fluid and solid nanoparticles, respectively.

The effective density is;
$$\rho_{nf} = (1-\phi)\rho_f + \phi\rho_p \tag{14}$$

The heat capacity is;
$$(\rho C_p)_{nf} = (1-\phi)(\rho C_p)_f + \phi(\rho C_p)_p \tag{15}$$

The effective thermal conductivity is;
$$\frac{k_{nf}}{k_f} = \frac{k_p + 2k_f + 2(k_p - k_f)(1 + \eta)^3 \phi}{k_p + 2k_f - (k_p - k_f)(1 + \eta)^3} \tag{16}$$

The Yu and Choi model was used for the thermal conductivity of the nanofluid. Parameter value in the equation; the ratio of the thickness of the liquid layer to the radius is taken as $\eta = 0.1$.

The viscosity is;
$$\mu_{nf} = \frac{\mu_f}{(1-\phi)^{2.5}} \tag{17}$$

The Brinkman model was used to determine the viscosity of the nanofluid.

Numerical Solution Method

In this study, the continuity, momentum and energy equations are solved using ANSYS FLUENT CFD software, which is based on the finite volume method. The problem is considered as two-dimensional and the flow is accepted to be turbulent and the k-ε standard turbulent model is used. The finite volume method has been used to discretize the executive equations of flow, using the SIMPLEC algorithm to couple the pressure-velocity system. Second order upwind scheme and structure, uniform grid system have been employed to discretize the executive equation. The solutions are considered converged when the normalized residual values reach (10^{-5}) for all variables.

Compared with the results of the numerical and experimental study done by Abed et al. (2015). The comparison of the results of analysis of the present and reference study of Nusselt number with the different Re numbers of Al₂O₃-water nanofluid with solid volume ratio of $\phi = 0.04$ is presented in Table 2. It has been found that there is a good fit between the results obtained.

Table 2. Comparison of present and literature results of average Nusselt value for different Reynolds numbers.

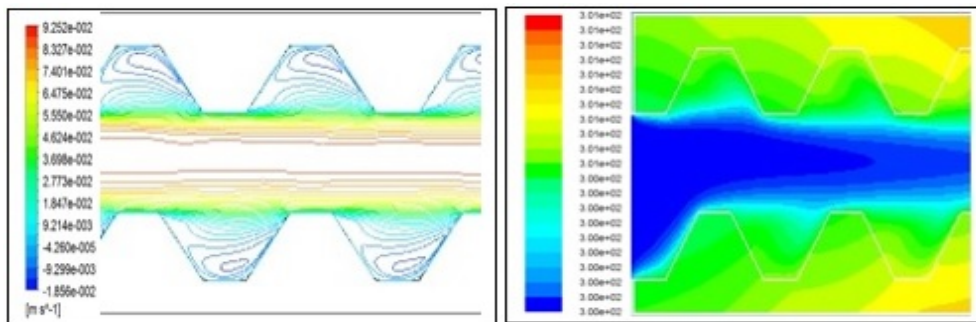
Re	6000	8000	12000	16000	20000
Mevcut	44.61	48.94	65.23	84.68	102.41
Abed vd. [15]	75.13	83.80	95.96	105.53	117.39

Results and Discussion

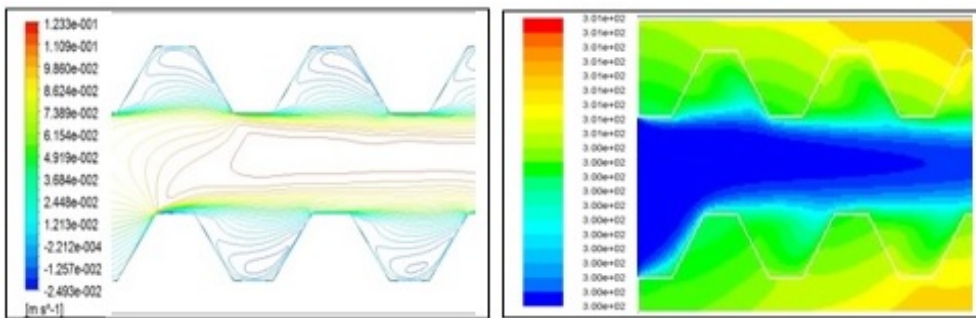
As working intervals in numerical analysis; the effects of Al₂O₃ nanoparticles with different base fluids (water, ethylene glycol, mercury and propane) and diameter $d = 20$ nm at different solid volume ratios ($\phi = 0\% - 4\%$) under constant heat flow ($q = 6 \text{ kW} / \text{m}^2$). Geometric parameters of the trapezoidal channel; trapezoidal height is $e = 5$ mm, trapezoidal pitch is $Pe = 12$ mm, width of the top trapezoidal channel is $w = Pe/4 = 3$ mm. The length of the heat source ($w = L$) and total width of channel was used as the non-dimensional distance $D / L = 0.21$ ($D = 20.5\text{mm}$) of the heat source from the right and left adiabatic walls.

Fig.2 shows that velocity distributions on the left and isotherm contours on the right of the mercury based nanofluid at different Reynolds numbers and $\phi = 0.04$ volume fraction. As the number of Reynolds increases, the circulation increases and flow velocity profiles appear in the vortex appearance in the regions near the wall of the corrugated trapezoidal channel. As the Reynolds number and the solid volume ratios increase, the velocity increases. Accordingly, as the velocity increases, the circulation regions begin to grow laterally along the corrugated channel cavities, and flow structures is not disturbed by corrugated channel. In terms of isotherm countours, it increases

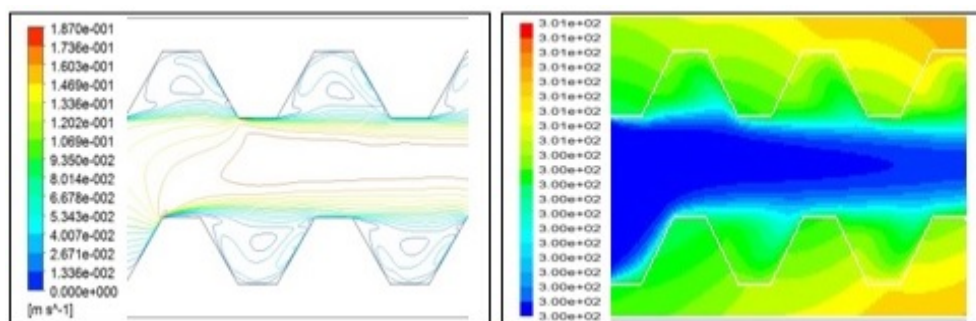
the flow temperature of the corrugated channel walls more because of the low velocity value due to the viscosity of the nanofluid. It is observed that the cold fluid is uniform at the lower boundary of the channel grooves in the central region. As the Reynolds number increases, thermal boundary layers develop near the walls. The nanofluid supports the mixing of the hot fluid near the thermal boundary layer and the cold fluid in the central region. The beginning and growth of the circulation flow allows mixing of the fluid in the central region with the hot fluid near the boundary layer. The flow is determined in a groove which forms a secondary circulation flow. As the Reynolds number increases, the thermal boundary layer thickness decrease. The reverse flow occurs in the groove near the upper and lower walls of the corrugated channel. As the Reynolds number increases, the velocity in the groove near the walls in the opposite direction of the main flow increases. The density of secondary flow increases for main flow and the size of the circulation region increases. Then, the circulation flow becomes even more turbulent. Temperature gradients increase with increasing Reynolds number due to the circulation flow occurred near the corrugated wall.



Re=6000



Re=8000



Re=12000

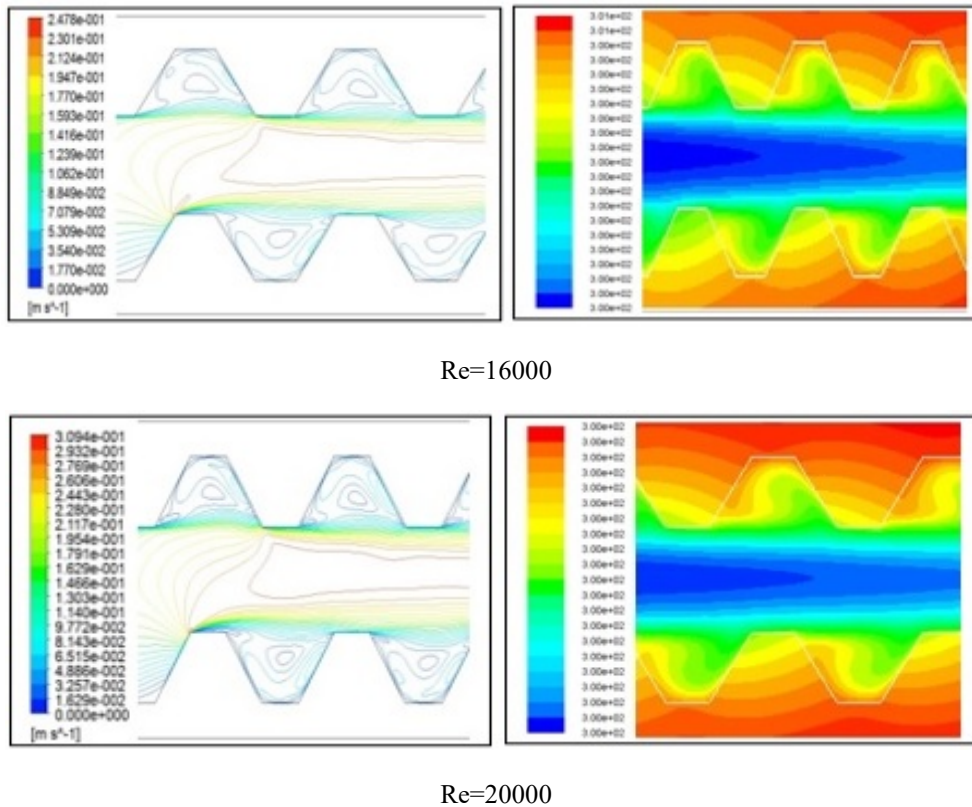
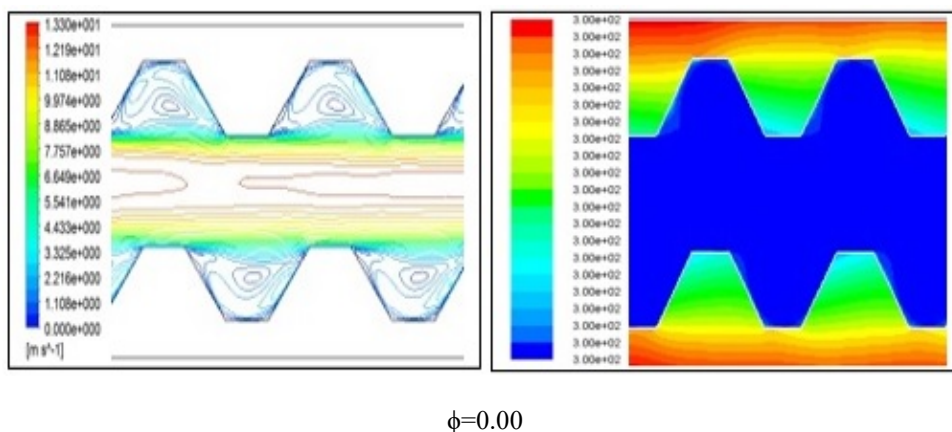
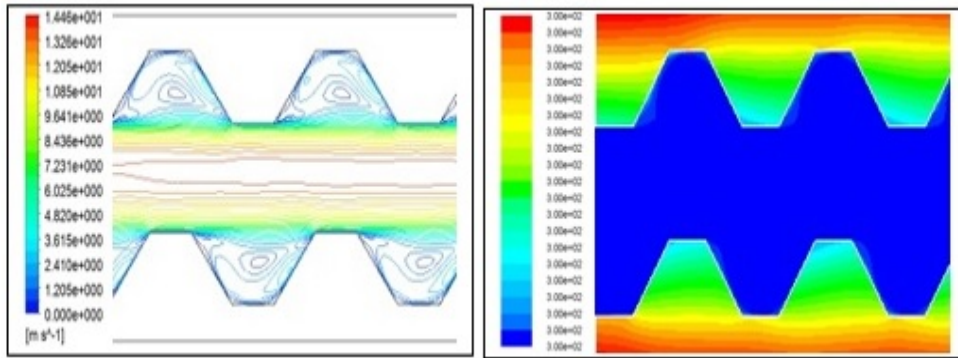


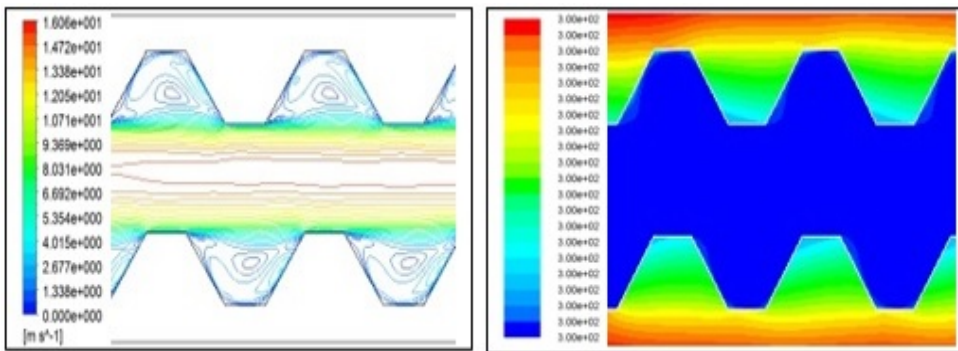
Fig. 2. Velocity distribution (left) and isotherms (right) contours of the mercury based nanofluid at different Reynolds numbers and volume fraction $\phi=0.04$.

Fig.3 shows that velocity distribution on the left and isotherm contours on the right of the ethylene glycol based nanofluid at $Re=12000$ and different volume fractions. With the Brownian action, the rates of nanoparticles added to the base fluid ethylene glycol increase, increasing volume fraction. In terms of isotherm contours, the temperature gradient increases with the increase of volume fraction by the addition of nanoparticles having high thermal conductivity with respect to the base fluid. When the velocity distribution and isotherm contours are compared to ethylene glycol with a high Prandtl number and mercury with a lower Prandtl number; as the Prandtl number increases, the inlet velocities of the fluid increase, so the circulation increases and the thermal boundary layers become thinner.

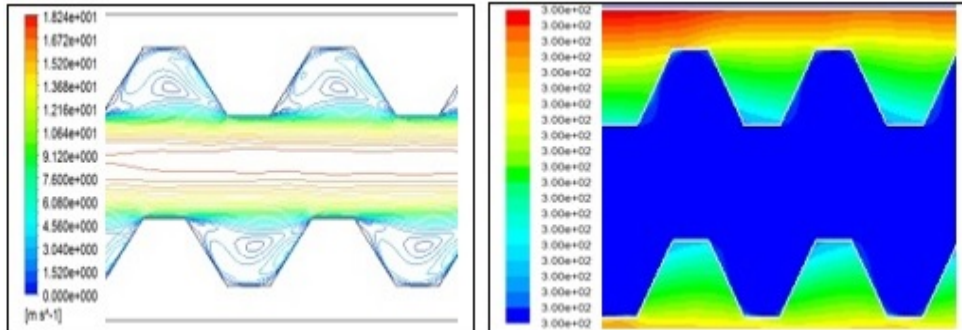




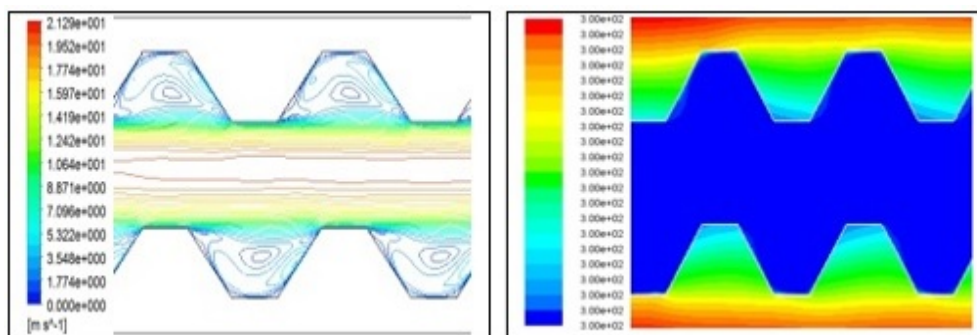
$\phi=0.01$



$\phi=0.02$



$\phi=0.03$



$\phi=0.04$

Fig. 3. Velocity distribution (left) and isotherms (right) contours of the ethylene glycol based nanofluid at $Re=12000$ and different volume fractions.

Fig.4. shows that the average Nusselt number on the left and pressure drops on the right of water, ethylene glycol, mercury, propane based fluids at different Reynolds numbers and volume fraction $\phi=0.04$. Since the viscosity of the ethylene glycol based nanofluid is higher than water, mercury and propane based nanofluids, the velocity values and hence the temperature change are increasing. In this case, both the average Nu number and the pressure drops higher values were obtained.

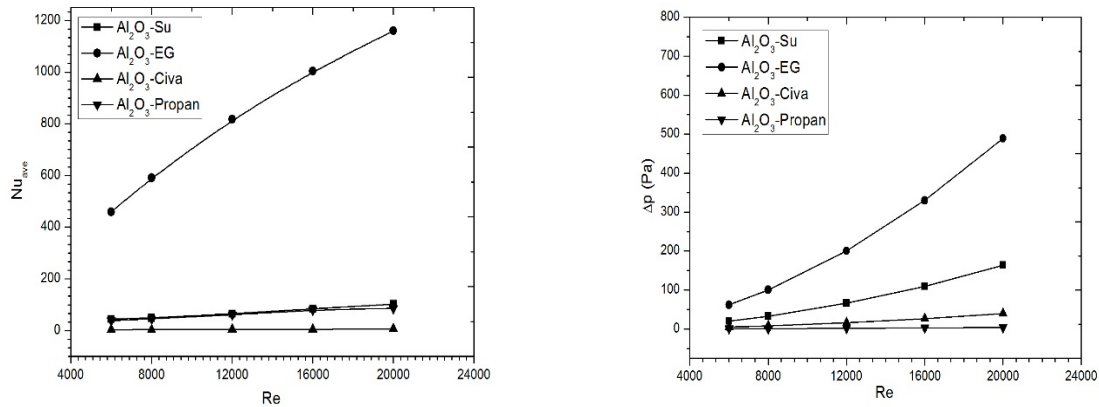


Fig. 4. Effect of various base fluids with different Reynolds numbers on the average Nusselt number (left) and the pressure drops (right) volume fraction $\phi=0.04$.

Fig.5. shows that the average Nusselt number on the left and pressure drops on the right of Al_2O_3 -water nanofluid at different Reynolds numbers and volume fractions. Accordingly, both the average Nusselt number and the pressure drop increase with increasing Reynolds number and volume fraction.

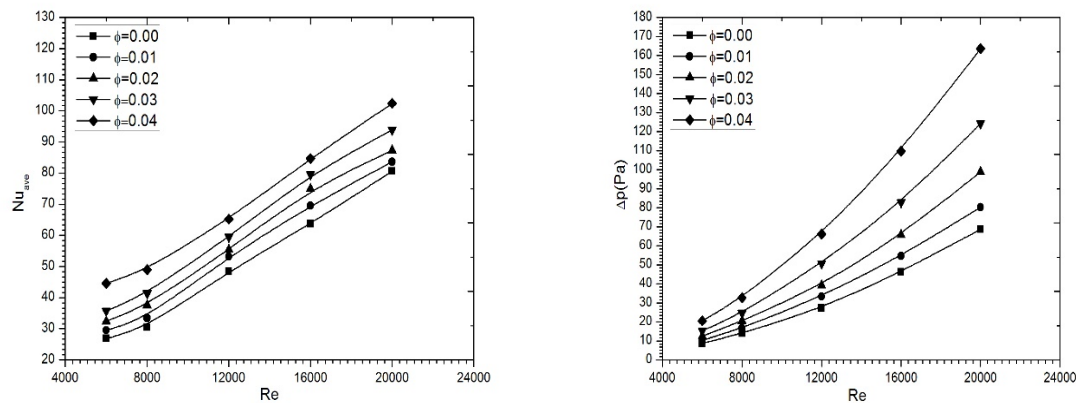


Fig. 5. Effect of Al_2O_3 -water nanofluid on the average Nusselt number (left) and the pressure drops (right) at different Reynolds number and volume fractions

The average Nusselt values of the different base fluids and nanofluids with different volume fractions obtained from the studies in the numerical analyzes are presented in Table 3. Accordingly, the average Nusselt number, increases as the solid volume ratio of the nanoparticles increases. As a result of increasing Reynolds number, high velocity values are obtained and the average Nusselt values increase. The temperature difference from the analyzes affects the average h_c heat transfer coefficient along the corrugated trapezoidal channel. When different base fluid of nanofluids were compared, the highest average Nusselt value was obtained with ethylene glycol based nanofluid

and the lowest the average Nusselt value was obtained with mercury based nanofluid. The propane based nanofluid has been observed to be close to the water based nanofluid. That is, as Prandtl number increases, the average amount of heat transfer increases.

Table 3. Comparison of the average Nu numbers of different Reynolds numbers, Prandtl numbers and volume fractions

Re	ϕ	Al ₂ O ₃ -Mercury (Pr=0.0251)	Al ₂ O ₃ -Propane (Pr=2.87)	Al ₂ O ₃ -water (Pr=6.07)	Al ₂ O ₃ -EG (Pr=137.48)
6000	0.00	3.23	25.85	26.89	385.22
	0.01	3.26	27.57	29.52	393.93
	0.02	3.28	29.92	32.43	407.38
	0.03	3.33	31.32	35.71	429.72
	0.04	3.42	38.17	44.61	458.82
8000	0.00	3.37	26.68	30.45	492.76
	0.01	3.42	32.88	33.45	510.09
	0.02	3.50	36.74	37.47	527.30
	0.03	3.61	39.25	41.35	553.59
	0.04	3.77	45.71	48.95	590.86
12000	0.00	3.78	39.01	48.42	702.46
	0.01	3.90	40.03	53.18	716.15
	0.02	4.03	52.76	55.39	749.60
	0.03	4.23	54.61	59.47	771.33
	0.04	4.48	61.23	65.23	817.49
16000	0.00	4.23	50.26	63.72	873.65
	0.01	4.39	57.74	69.54	889.46
	0.02	4.59	63.12	74.96	915.14
	0.03	4.84	70.92	79.62	953.29
	0.04	5.16	79.65	84.69	1003.51
20000	0.00	4.69	69.20	80.61	1018.67
	0.01	4.87	77.57	83.64	1037.54
	0.02	5.09	78.63	87.24	1064.45
	0.03	5.40	84.95	93.88	1106.48
	0.04	5.80	86.92	102.41	1159.49

Conclusions

In this study, fully developed turbulent forced convective flow and heat transfer behavior of the nanofluid containing water, ethylene glycol, mercury and propane based Al_2O_3 nanoparticles in a two-dimensional corrugated trapezoidal plate heat exchanger have been numerically investigated. Corrugated trapezoidal channel constant heat flow boundary condition was applied. According to the results obtained; adding nanoparticles to base fluids increases heat transfer. It is also seen that the heat transfer is increased by increasing the volume fraction of the nanofluid. As the concentration of nanoparticles increases, the average Nusselt number and pressure drop increase. When the base fluids were compared, the highest average Nu and pressure drop were obtained with ethylene glycol based nanofluid and the lowest value with mercury based nanofluid. On the other hand, the increase of Prandtl number causes the heat to spread more slowly than the momentum. The heat transfer is significantly affected. Compared analyzes made with pure water as the base fluid, the increase in pressure loss in the case where volume fraction of the water-based nanofluid is 4% and the Reynolds number is 20000 is about 2.4 times as high. The average Nusselt number has improved by around 13%. It was observed that the water-based nanofluid is higher but close to the propane-based nanofluidic values. The following findings can be written:

- There is no study that has focused on convective heat transfer by nanofluid through corrugated trapezoidal channel step.
- The utilization of nanofluids in the corrugated channels has augmented the heat transfer with slight pressure drop.
- The enhancement of heat transfer potential of the base fluids in the corrugated trapezoidal channels will offer an opportunity for engineers to develop highly compact and effective heat transfer equipment for many industrial applications.
- The benefit of the utilization of nanofluids in the new channels is used in many applications including transportation, the electronic cooling systems, the chemical processes, the combustion chambers, the cooling of turbine blades, the environmental control systems and the high performance heat exchangers.
- It is necessary to study the development of correlations of friction factor and Nusselt number in the corrugated trapezoidal channels with nanofluids.

References

- Abed, A.M., Alghoul, M.A., Sopian, K., Mohammed, H.A., Majdi, H. & Al-Shamani, A.N. (2015). Design characteristics of corrugated trapezoidal plate heat exchangers using nanofluids, *Chemical Engineering and Processing*, 87 (pp.88–103).
- Ahmed, M.A., Shuaib, N., Yusoff, M. & Al-Falahi, A. (2011). Numerical investigations of flow and heat transfer enhancement in a corrugated channel using nanofluid, *Int. Commun. Heat Mass Transfer*, 38 (pp.1368–1375).
- Ahmed, M.A., Yusoff, M.Z., Ng, K.C. & Shuaib, N.H. (2015). Numerical and experimental investigations on the heat transfer enhancement in corrugated channels using SiO_2 -water nanofluid, *Case Studies in Thermal Engineering* 6 (pp.77–92).
- Choi, S-S. (1995). Enhancing thermal conductivity of fluids with nanoparticles, *Develop. Appl. Non Newtonian Flows* (pp.99–106).
- Esmaceli, M., Sadeqy, K. & Moghaddami, M. (2010). Heat transfer enhancement of wavy channels using Al_2O_3 nanoparticles. *J Enhancement Heat Transfer*, 17(2), (pp.139).
- Heidary, H. & Kermani, M. (2010). Effect of nano-particles on forced convection in sinusoidal-wall channel, *Int. Commun. Heat Mass Transfer*, 37 (pp.1520–1527).
- Heidary, H. & Kermani, M. (2012). Heat transfer enhancement in a channel with block (s) effect and utilizing nanofluid, *Int. J. Therm. Sci.*, 57 (pp.163–171).
- Islamoglu, Y., & Parmaksizoglu, C. (2003). The effect of channel height on the enhanced heat transfer characteristics in a corrugated heat exchanger channel, *Appl. Therm. Eng.*, 23 (pp.979–987).
- Kebliński, P., Phillpot, S.R., Choi, S-S., & Eastman, J.A. (2002). Mechanisms of Heat Flow in Suspensions of Nano-sized Particles (nanofluids), *Int. J. Heat Mass Transfer*, 45 (pp.855–863).
- Kwon, H.G., Hwang, S.D., Cho, H.H. (2008). Flow and heat/mass transfer in a wavy duct with various corrugation angles in two dimensional flow regimes, *Heat Mass Transfer*, 45 (pp.157–165).
- Lee, S., Choi, S-S., Li, S., & Eastman, J.A. (1999). Measuring thermal conductivity of fluids containing oxide nanoparticles, *ASME J. Heat Transfer*, 121 (pp.280-289).
- Mohammed, H., Abed, A.M., & Wahid, M. (2013). The effects of geometrical parameters of a corrugated channel with in out-of-phase arrangement, *Int. Commun. Heat Mass Transfer*, 40 (pp.47-57).

- Navaei,A.S., Mohammed,H.A., Munisamy,K.M., Yarmand,H. & Gharehkhani,S. (2015). Heat transfer enhancement of turbulent nanofluid flow over various types of internally corrugated channels, *Power Tecnology* (pp.332–341).
- Naphon,P. (2007). Laminar convective heat transfer and pressure drop in the corrugated channels, *Int. Commun. Heat Mass Transfer*,34 (pp.62–71).
- Naphon,P. (2009). Effect of wavy plate geometry configurations on the temperature and flow distributions, *Int. Commun. Heat Mass Transfer*,36 (pp.942–946).
- Ozbolat ,V. & Sahin,B. (2013). Numerical investigations of heat transfer enhancement of water-based Al₂O₃ nanofluids in a sinusoidal-wall channel. *ASME International Mechanical Engineering Congress and Exposition. American Society of Mechanical Engineers*,(V08AT09A051-V08AT09A051).
- Pantzali,M., Mouza,A. & Paras,S. (2009). Investigating the efficacy of nanofluids as coolants in plate heat exchangers (PHE), *Chem. Eng. Sci.*,64 (pp.3290–3300).
- Rostami,J. (2007) Convective heat transfer in a wavy channel utilizing nanofluids. *J Enhancement Heat Transfer* (pp.14-52).
- Tanda,G. (2007). Heat transfer in rectangular channels with transverse and V-shaped broken ribs, *Int. J. Heat Mass Transfer*,47 (pp.229–243).
- Tiwari,A.K., Ghosh,P., Sarkar,J., Dahiya,H. & Parekh,J. (2014). Numerical investigation of heat transfer and fluid flow in plate heat exchanger using nanofluids, *Int. J. Therm. Sci.*,85 (pp.93–103).